

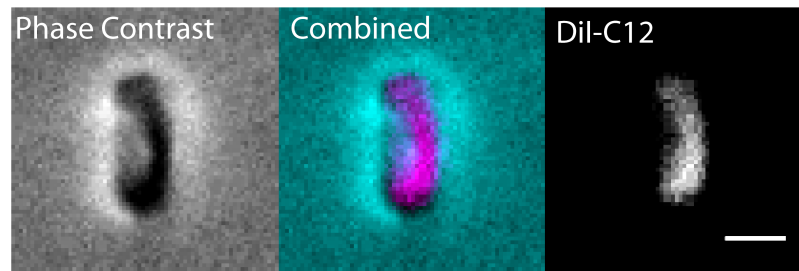
Biophysical Journal, Volume 110

Supplemental Information

**MreB-Dependent Organization of the *E. coli* Cytoplasmic Membrane
Controls Membrane Protein Diffusion**

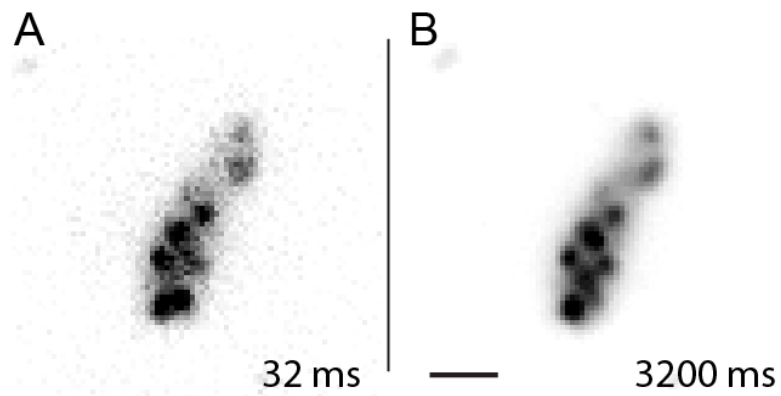
**Felix Oswald, Aravindan Varadarajan, Holger Lill, Erwin J.G. Peterman, and Yves J.M.
Bollen**

Supplementary Fig. 1



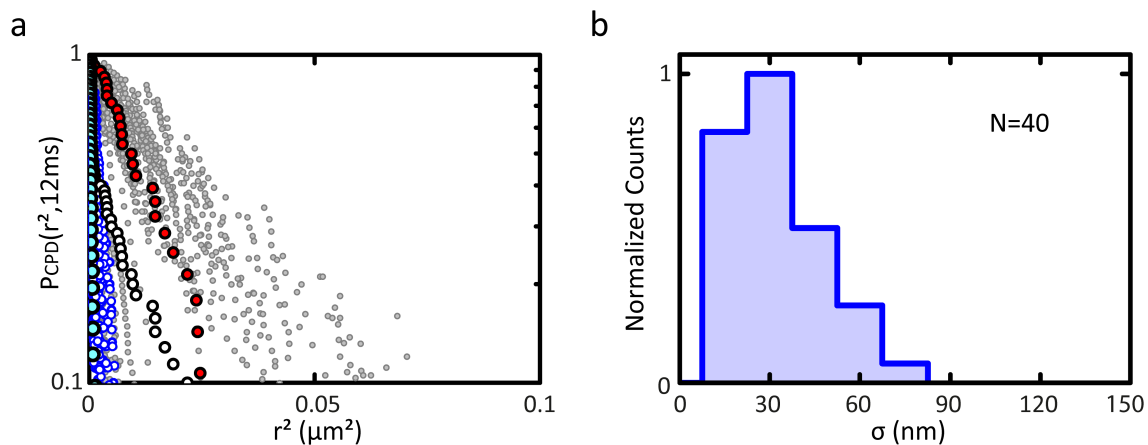
Supplementary Fig. 1. Plasmolysis of a DiI-C12 stained *E.coli* cell. Left: Image obtained by phase contrast. The dark area shows the deformed high-refractive cytoplasm that has detached from the cell wall due to plasmolysis. Right: Fluorescence image of DiI-C12 displays the same deformation, indicating that DiI-C12 exclusively stains the cytoplasmic membrane of *E.coli*. Middle: the overlay of phase-contrast (cyan) and fluorescence (magenta) images shows that the cytoplasmic and DiI-C12 stained areas match. Scale bar: 1 μm .

Supplementary Fig. 2



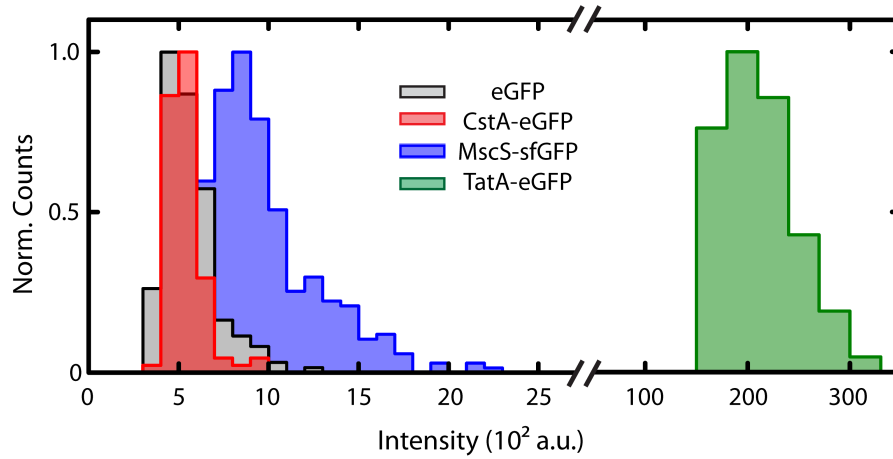
Supplementary Fig. 2 Stable DiI-C12 micro-domains also form at 37°C. *E. coli* cells were grown and imaged at 37°C. (A) single frame of 32 ms. (B) time-averaged image (100 frames). Scale bar: 1 μm.

Supplementary Fig. 3



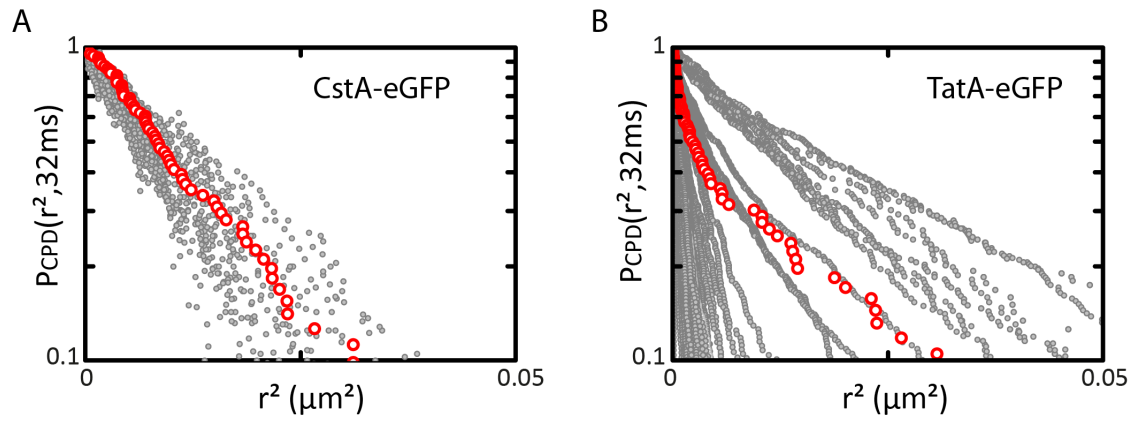
Supplementary Fig. 3 Estimation of DiI-C12 domain sizes. (a) CPDs of long single-molecule trajectories of DiI-C12 with low-mobility trajectories highlighted in dark blue. Highlighted in black a CPD of the mobility-switching DiI-C12 molecule shown in Supplementary Movie 4, with the CPD of its mobile stretch highlighted in red and the CPD of its immobile stretch highlighted in cyan. (b) Distribution of the standard deviation of localizations of low-mobility DiI-C12 molecules as an estimate of DiI-C12 domain size.

Supplementary Fig. 4



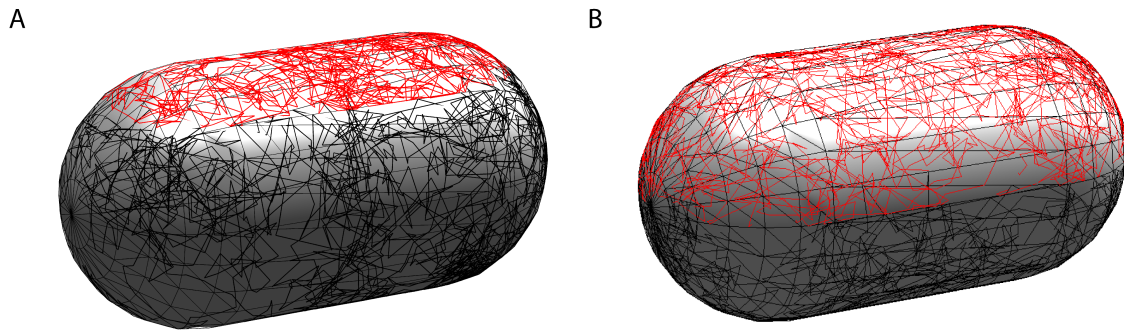
Supplementary Fig. 4 Intensity distributions of purified eGFP measured *in vitro* and CstA-eGFP, MscS-sfGFP, TatA-eGFP obtained *in vivo*. Mean intensity of monomeric CstA-eGFP ($I_{mean} = 520 \pm 80$ a.u., N=132) and purified eGFP ($I_{mean} = 510 \pm 150$ a.u., N=183) match within the standard deviation. MscS-sfGFP displays a broader distribution ($I_{mean} = 920 \pm 30$ a.u., N=201) indicating that multiple MscS-sfGFP incorporate in pentameric complexes with unlabelled wild-type MscS. The mean eGFP intensity was used to select for TatA-eGFP multimers that incorporate at least 30 monomers yielding a distribution with an average complex size of 38.4 ± 6.6 monomers ($I_{mean} = 196.8 \cdot 10^2 \pm 34 \cdot 10^2$ a.u., N=63).

Supplementary Fig. 5



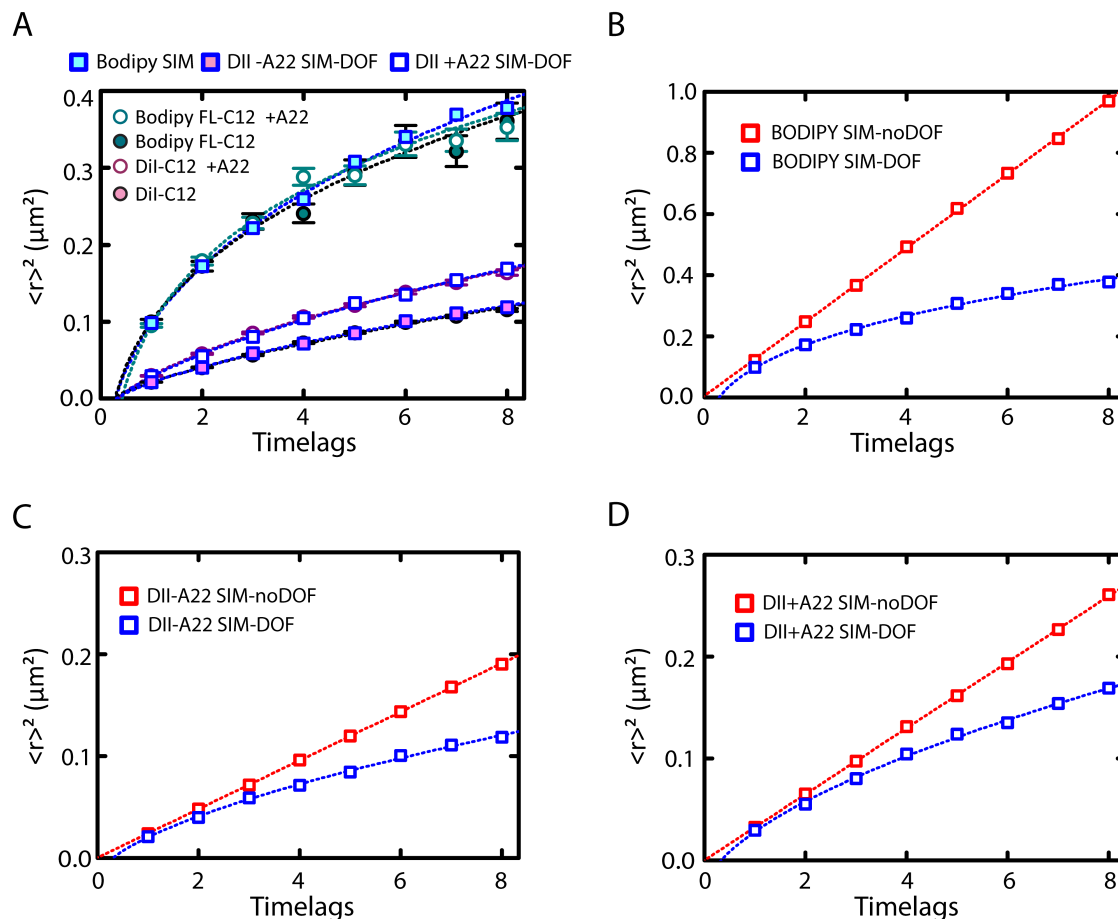
Supplementary Fig. 5. CPDs of 3D-corrected long single-molecule trajectories of CstA-eGFP (A) and TatA-eGFP (B). Highlighted CPDs correspond to trajectories visualized in Supplementary Movie 5 and Supplementary Movie 7.

Supplementary Fig. 6



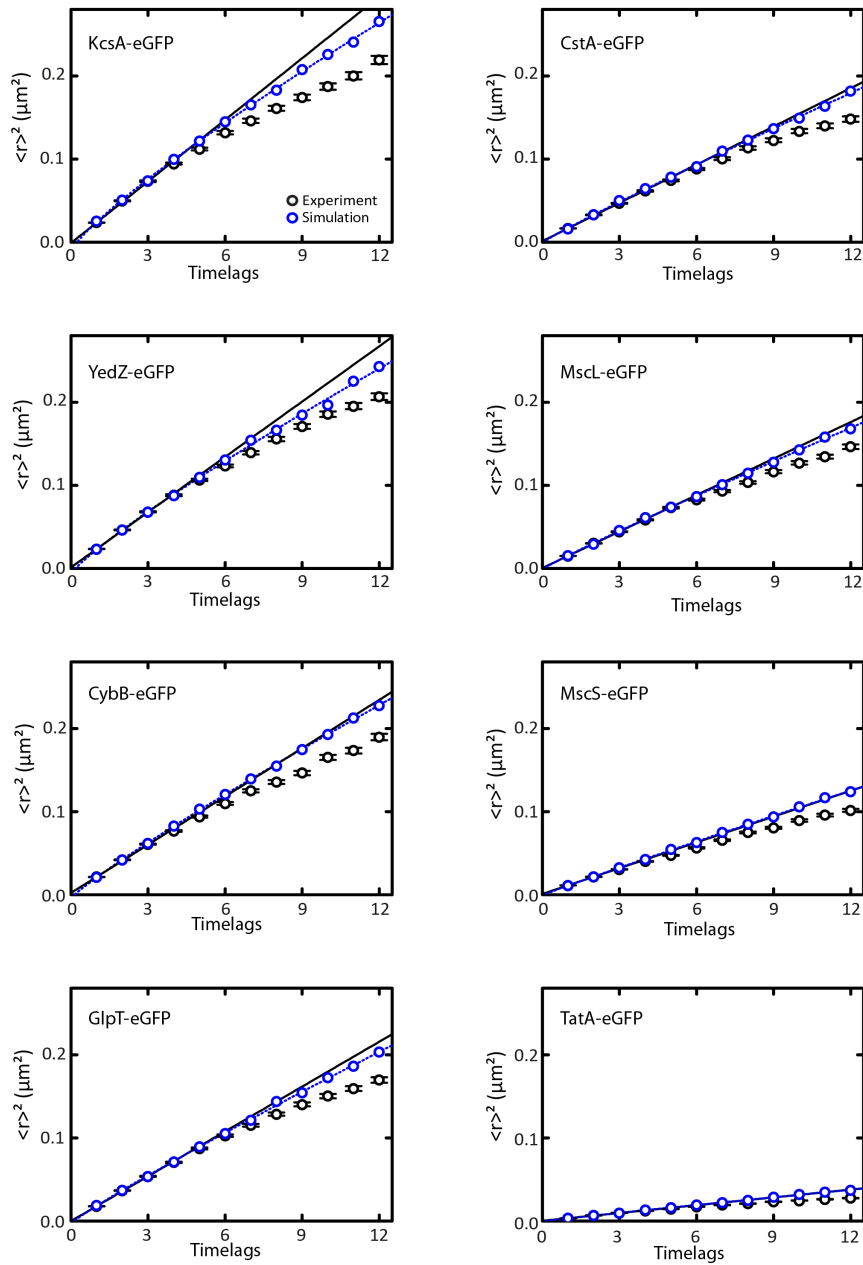
Supplementary Fig. 6. Illustration of depth-of-field (DOF) simulation for TIRF (A) and epi (B) imaging conditions. Brownian motion simulated along the bacterial surface model with accepted displacements occurring within the DOF in red and discarded displacements in black.

Supplementary Fig. 7



Supplementary Fig. 7. Long-time MSD analysis of lipid-dye mobility and the effect of the limited depth of field. (A) Experimental long time-lag MSDs of Bodipy FL-C12 and DiI-C12 in presence and absence of A22 indicated by circles as shown in the legend. MSDs of Brownian motion simulation assuming experimental diffusion constants and considering the limited DOF under TIRF conditions indicated by squares. (B),(C),(D) MSD plots of diffusion simulations considering (blue) and without considering (red) TIRF DOF. Note that the blue curves and symbols are also shown in (A).

Supplementary Fig. 8



Supplementary Fig. 8. Long-time MSD analysis of TMP mobility. Black solid lines represent linear fits to only the first 4 time lags of experimental MSDs (black circles). Blue dashed lines represent nonlinear fits to MSDs of diffusion simulations (blue circles) assuming diffusion constants obtained from linear fits to the first 4 time lags and a DOF under EPI conditions.

Supplementary Table 1

Protein	Mean Intensity (10^2 a.u.)	Number (eGFP)
eGFP	5.1±1.5	1.0±0.2
WALP-KcsA-eGFP	4.8±0.8	1.0±0.2
YedZ-eGFP	5.1±1.3	1.0±0.3
CybB-eGFP	5.6±1.2	1.1±0.2
GlpT-eGFP	5.2±0.8	1.0±0.2
CstA-eGFP	5.2±0.8	1.0±0.2
MscL-eGFP	7.2±1.9	1.4±0.4
MscS-sfGFP	9.2±3.0	1.8±0.6
TatA-eGFP	196.8±33.9	38.4±6.6

Supplementary Table 1. Mean values of intensity distributions obtained *in vitro* for purified eGFP and *in vivo* for GFP-tagged trans-membrane proteins. The mean intensity of eGFP was used to estimate the number of TMP-GFP monomers in analysed single-particle trajectories. Values are given with the corresponding standard deviation of the underlying intensity distributions.

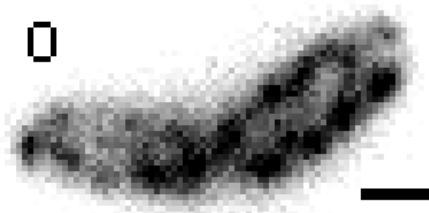
Supplementary Table 2

TM-Protein/ Lipid-Dye	Radius (nm)	D_1 ($\mu\text{m}^2/\text{s}$)	D_2 ($\mu\text{m}^2/\text{s}$)	γ
WALP-KcsA- eGFP	0.9	0.196 ± 0.002	-	-
YedZ-eGFP	1.3	0.186 ± 0.001	-	-
CybB-eGFP	1.7	0.168 ± 0.001	-	-
GlpT-eGFP	2.0	0.137 ± 0.001	-	-
CstA-eGFP	2.3	0.130 ± 0.001	-	-
CstA-eGFP +A22	2.3	0.193 ± 0.003	-	-
MscL-eGFP	2.5	0.114 ± 0.001	-	-
MscS-sfGFP	4.0	0.080 ± 0.001	-	-
TatA-eGFP	6.5	0.016 ± 0.001	0.176 ± 0.004	0.90 ± 0.01
Bodipy FL- C12	-	1.649 ± 0.057	-	-
Bodipy FL- C12+A22	-	1.475 ± 0.062	-	-
DiI-C12	-	0.029 ± 0.008	0.584 ± 0.007	0.49 ± 0.01
DiI-C12+A22	-	0.006 ± 0.090	0.617 ± 0.020	0.17 ± 0.06

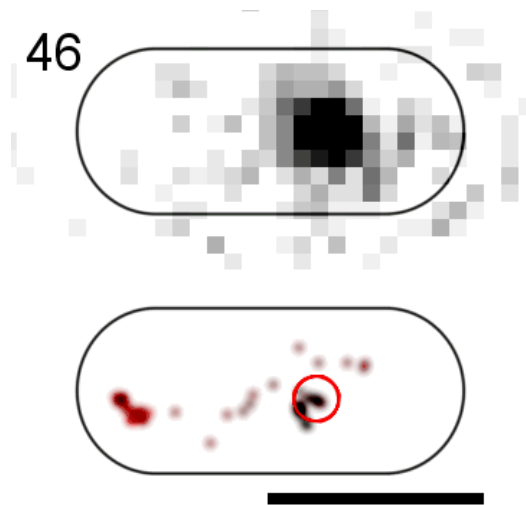
Supplementary Table 2 CPD analysis of TMP and lipid-dye diffusion. In case of TatA-eGFP and DiI-C12, double-exponential fits yield two populations with two distinct diffusion constants D_1 and D_2 with the relative occurrence γ .



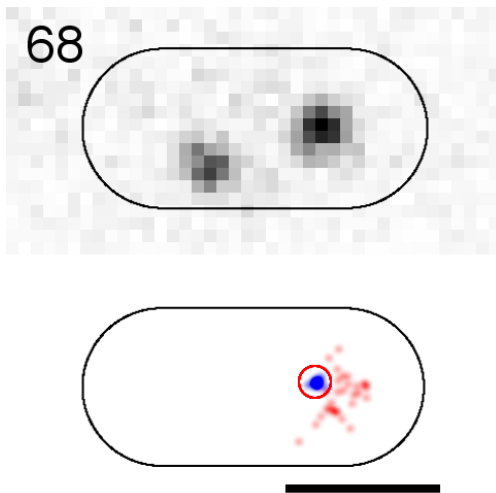
Supplementary Movie 1. Movie of *E.coli* stained with DiI-C12 observed with continuous epifluorescence illumination and 32ms exposure time per frame. Scale bar: 1 μ m.



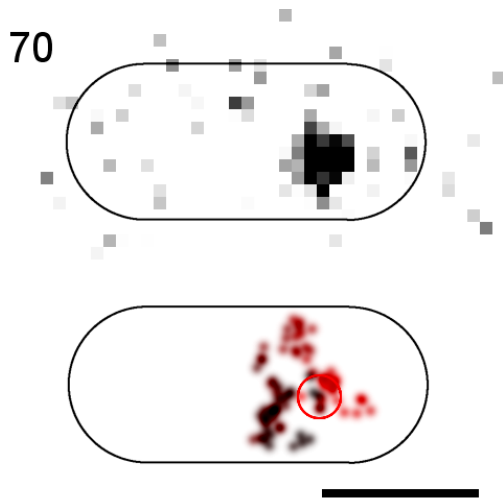
Supplementary Movie 2. Movie of *E.coli* stained with DiI-C12 in presence of A22 observed with continuous epi-fluorescence illumination and 32ms exposure time per frame. Scale bar: 1 μ m.



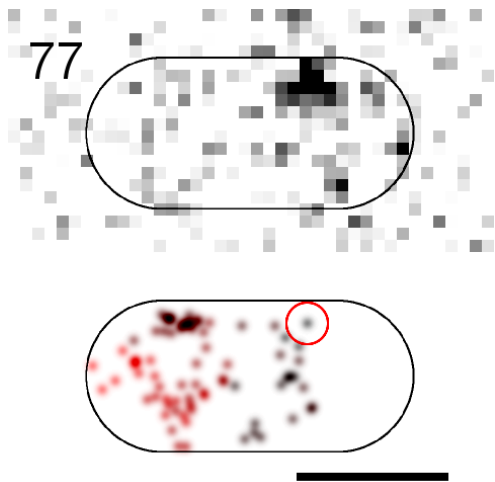
Supplementary Movie 3. Movie of a DiI-C12 single-molecule trajectory (depicted in Fig. 3c) observed with continuous TIRF-fluorescence illumination and 12ms exposure time per frame. Top: raw images. Bottom: 2D-Gaussian-rendered single-molecule positions of the trajectory. Scale bar: 1 μ m.



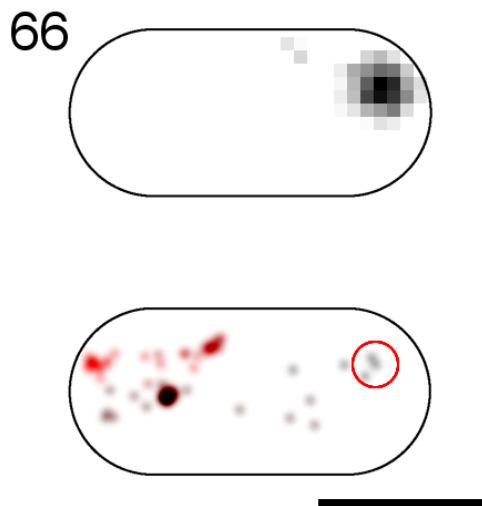
Supplementary Movie 4. Movie of a DiI-C12 mobility switching single-molecule trajectory observed with continuous TIRF-fluorescence illumination and 12ms exposure time per frame. Bottom: raw images. Top: 2D-Gaussian-rendered single-molecule positions of the trajectory with its mobile stretch in red and immobile stretch in blue. Scale bar: 1 μm .



Supplementary Movie 5. Movie of a CstA-eGFP single-molecule trajectory (depicted in Fig. 4c) observed with continuous epi-fluorescence illumination and 32ms exposure time per frame. Top: raw images. Bottom: 2D-Gaussian-rendered single-molecule positions of the trajectory. Scale bar: 1 μm .



Supplementary Movie 6. Movie of a CstA-eGFP single-molecule trajectory in presence of A22 (depicted in Fig. 4d) observed with continuous epi-fluorescence illumination and 32ms exposure time per frame. Top: raw images. Bottom: 2D-Gaussian-rendered single-molecule positions of the trajectory. Scale bar: 1 μ m.



Supplementary Movie 7. Movie of a TatA-eGFP single-molecule trajectory observed with continuous epi-fluorescence illumination and 32ms exposure time per frame. Top: raw images. Bottom: 2D-Gaussian-rendered single-molecule positions of the trajectory. Scale bar: 1 μ m.